Available online at www.sciencedirect.com
ScienceDirect
Scripta Materialia 64 (2011) 1011–1014
Scripta MATERIALIA
www.elsevier.com/locate/scriptamat

Graded phase structure in the surface layer of NiTi alloy processed by surface severe plastic deformation

T. Hu,[a,b] L. Chen,[b] S.L. Wu,[a] C.L. Chu,[c,*] L.M. Wang,[b] K.W.K. Yeung[d] and Paul K. Chu[a,*]

[a]*Department of Physics & Materials Science, City University of Hong Kong, Tat Chee Avenue, Kowloon, Hong Kong*
[b]*Department of Nuclear Engineering and Radiological Science, The University of Michigan, Ann Arbor, MI 48109, USA*
[c]*School of Materials Science and Engineering, Southeast University, Nanjing 211189, China*
[d]*Department of Orthopaedics & Traumatology, The University of Hong Kong, Pokfulam Road, Hong Kong*

Received 30 November 2010; revised 6 February 2011; accepted 9 February 2011
Available online 12 February 2011

The graded phase structure and its evolution in the surface of NiTi alloy after surface mechanical attrition treatment are studied using transmission electron microscopy. The initial B2–B19′ phase transformation occurs at low strain level. As the deformation strain increases, the B19′ martensite phase transforms back to B2 phase giving rise to graded phases. Our study reveals that stress induced martensite transformation and deformation heating play important roles in the formation of this graded phase structure.

Keywords: Graded phase; Nanocrystalline; NiTi alloy; Deformation heating; Surface mechanical attrition treatment

Severe plastic deformation (SPD) is an effective method to produce surface nanocrystalline structures [1,2]. After undergoing SPD, nanocrystalline materials have extraordinary properties, including high strength, enhanced hardness and diffusion coefficients superior to those of their coarse-grained counterparts [3–6]. To further improve the mechanical properties, recent research has been focussed on the grain size and its distribution, the underlying mechanism of grain refinement, as well as the compromise between strength and ductility [5,7,8]. Systematic studies have been mainly performed on pure metals, e.g. Cu, Fe, Ti, Co and Zr [5,9–11]; however, most engineering materials have dual/multiple phases or are intermetallic compounds. The mechanical properties of these materials are determined not only by the grain size, but also by the phase constituents and their evolution during processing. However, few investigations have been performed on the phase transformation and evolution in alloys or intermetallic compounds with nanocrystalline structures and refined grains. In order to obtain engineering nanocrystalline materials, it is imperative that the phase transformation behavior in multiphase alloys or intermetallic compounds is better understood.

NiTi shape memory alloys (SMAs) constitute a class of smart materials possessing the unique shape memory effect and pseudoelasticity [12,13]. The shape memory effect is based on the thermally elastic and reversible martensite transformation. The high-temperature B2 (austenite) phase transforms to B19′ (martensite) phase upon cooling below a specific temperature, producing a distorted monoclinic martensite structure. The B19′ phase is generated by stressing the metal in the B2 state and this B19′ phase is capable of large strain, yielding the pseudoelasticity. When the load is removed, the B19′ phase transforms back to the B2 phase, resuming its original shape. Therefore, NiTi SMA provides a suitable platform to study the phase transformation behavior under deformation and/or thermal treatment. In this study, NiTi SMA is subjected to SPD by surface mechanical attrition treatment (SMAT) to produce a graded phase structure on the surface. Microscopic studies disclose that the stress-induced martensite (SIM) transformation as well as deformation heating play important roles in the phase transformation behavior.

Commercial NiTi alloy plates containing 50.8 at.% Ni and 49.2 at.% Ti were supplied by Nitinol Device Company. The initiate phase was B2 austenite with transformation points $A_s = 234.5$ K and $A_f = 257$ K.

* Corresponding authors. Tel.: +852 34427724; fax: +852 34420542; e-mail addresses: clchu@seu.edu.cn; paul.chu@cityu.edu.hk

1359-6462/$ - see front matter © 2011 Acta Materialia Inc. Published by Elsevier Ltd. All rights reserved.
doi:10.1016/j.scriptamat.2011.02.008

The materials were first annealed to obtain homogeneous coarse grains ranging from 40 to 80 μm. Prior to SMAT, the NiTi plates were polished with sandpapers to grade 800 and then electrochemically polished to reduce residual stress resulting from mechanical polishing. The SMAT experiments were conducted at room temperature for different time durations at a vibration frequency of 20 kHz. Stainless steel balls 2 mm in diameter were employed in this study; the details of the apparatus and procedures can be found elsewhere [9,14,15]. After SMAT, the microstructure of the NiTi specimens treated for 60 min was examined by transmission electron microscopy (TEM) using a Philips CM20 microscope operated at 200 kV. High-resolution TEM (HR-TEM) was also conducted on JEOL 2100F and JEOL 3011 microscopes at 200 and 300 kV, respectively. Both plain-view and cross-sectional thin foils were prepared for TEM observation. The plan-view samples were prepared by slicing a thin sample parallel to the plane of the impacted surface, followed by polishing from the non-impacted side and thinning to perforation using a twin-jet polisher after a thin coating of transparent loctite had been applied to the impacted surface to prevent thinning of the impacted surface. After perforation, the loctite was removed by dissolution in acetone and rinsing with ethanol. The twin-jet electropolishing process was conducted at −20 °C using a mixture of 15% HNO_3 and 85% CH_3OH. The cross-sectioned samples were prepared by the following procedures. Two thin samples were bonded with the impacted surfaces facing each other using M-Bond 610 glue (Allied High Tech Products, CA). The sample was sliced perpendicularly along the plane of the impacted surface and the thin foil was mechanically ground down to a thickness of about 20 μm. Finally, the sample was ion milled near the bonding line using a Gatan PIPS at a small incident angle and room temperature. X-ray diffraction (XRD) was carried out on a Philips X'pert diffractometer with Cu K_α radiation ($\lambda = 0.154056$ nm) at room temperature.

The deformed structure in the NiTi is first studied at low strain. Figure 1 shows the highly dense dislocations due to dislocation slipping at a depth of about 230 μm below the treated surface. The selected-area electron diffraction (SAED) pattern displays the typical B2 lattice in the NiTi alloy. This B2 phase undergoes SIM transformation and reverse transformation during SMAT.

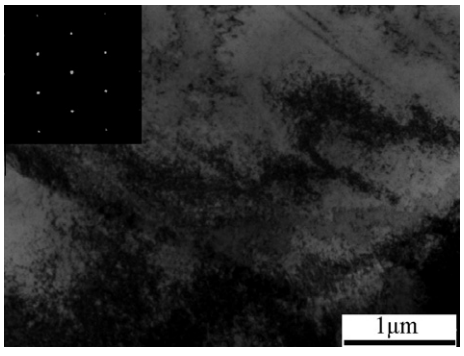

Figure 1. TEM image showing the high density of dislocations at a depth of about 230 μm in the SMAT NiTi specimen with the inset displaying the corresponding SAED pattern showing the B2 phase.

According to Jiang et al.'s study, dislocation would be generated in NiTi matrix to reduce the strain field during the reverse martensite transformation [16]. Therefore, it is inferred that the these observed highly dense dislocations are formed during the reverse martensite transformation. The formation of highly dense dislocations constitutes strain accommodation in the NiTi alloy deformed at low strain.

As the depth decreases, deformation strains increase. Figure 2 shows the phase structure at different strain levels after SMAT. At a depth of about 150 μm, martensite bands can be clearly seen (Fig. 2a1). These martensite bands are well oriented with widths of 40–200 nm and lengths of up to several micrometers. The results acquired by SAED show the B19′ phase (Fig. 2a2). The black and white bands originate from the B19′ phase, suggesting complete formation of the martensite phase at this depth, and the strain here is larger than that at the depth of 230 μm. The onset of the B2 → B19′ transformation at this depth is due to the SIM transformation during deformation.

Figure 2b1 shows the microstructure at a depth of 30 μm after SMAT. The specimen contains heterogeneously distributed and refined grains with nano and sub-micrometer sizes. The corresponding SAED pattern in Figure 2b2 shows the diffraction rings superimposed by diffraction spots. These diffraction rings stem from electron diffraction in the nanocrystalline and ultrafine grains. The diffraction pattern also shows traces of both the B2 and B19′ phases at this strain level. The results show that the B2 and B19′ phases coexist at a depth of about 30 μm, suggesting the occurrence of incomplete reverse martensite transformation (B19′ → B2) at high strain.

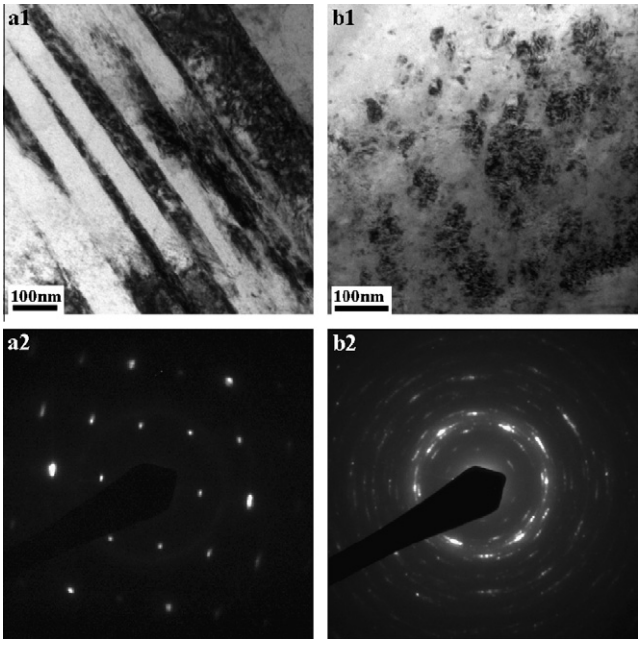

Figure 2. (a1) TEM image showing the martensite bands of SMAT NiTi at a depth of about 150 μm; (a2) SAED pattern taken from the TEM image in (a1); (b1) TEM image showing the microstructure of SMAT NiTi at a depth of about 30 μm; (b2) SAED pattern taken from TEM image in (b1) indicating the coexistence of the B19′ and B2 phases.